

Dynamic stabilization of a coupled ultracold atom-molecule system

Sheng-Chang Li^{1,*} and Chong Ye²¹*School of Science, Xi'an Jiaotong University, 710049 Xi'an, China*²*Graduate School, China Academy of Engineering Physics, 100088 Beijing, China*

(Received 18 August 2015; revised manuscript received 28 October 2015; published 29 December 2015)

We numerically demonstrate the dynamic stabilization of a strongly interacting many-body bosonic system which can be realized by coupled ultracold atom-molecule gases. The system is initialized to an unstable equilibrium state corresponding to a saddle point in the classical phase space, where subsequent free evolution gives rise to atom-molecule conversion. To control and stabilize the system, periodic modulation is applied that suddenly shifts the relative phase between the atomic and the molecular modes and limits their further interconversion. The stability diagram for the range of modulation amplitudes and periods that stabilize the dynamics is given. The validity of the phase diagram obtained from the time-average calculation is discussed by using the orbit tracking method, and the difference in contrast with the maximum absolute deviation analysis is shown as well. A brief quantum analysis shows that quantum fluctuations can put serious limitations on the applicability of the mean-field results.

DOI: [10.1103/PhysRevE.92.062147](https://doi.org/10.1103/PhysRevE.92.062147)

PACS number(s): 05.30.Jp, 03.75.Kk, 03.75.Mn, 67.85.-d

I. INTRODUCTION

The inverted pendulum is a typical example of the unstable equilibrium phenomena in classical mechanics, which represents a hyperbolic fixed point in the phase space corresponding to a metastable orientation of the pendulum. It is well known that even if a perfect preparation of the metastable orientation is initially possible, in reality both thermal fluctuations and unavoidable quantum fluctuations would still perturb the pendulum from the metastable orientation and lead to further dynamical evolution [1,2]. However, the unstable equilibria of physical systems can be dynamically stabilized by external periodic forcing. For the inverted pendulum, it can be stabilized by vibrating the pivot point (Kapitza's pendulum) [3]. The rapid advances in ultracold atomic physics over the past several decades provide opportunities to explore similar dynamical behavior in quantum many-body systems [4–6]. Dynamic stabilization of nonequilibrium Bose-Einstein condensate (BEC) has been suggested by changing the sign of the scattering length [7–10], tuning the spin-dependent interaction strength [11], and varying the trapping potential in a double-well BEC [12–14]. The nonequilibrium dynamics of an unstable quantum pendulum [15] and dynamic stabilization [16] in a spin-1 BEC have been investigated experimentally. The relevant study in this field has been used for controlling the superfluid-Mott insulator phase transition [17], and generating squeezed states [18–22] and non-Gaussian states [15], which are potential resources for quantum enhanced measurements [23] and quantum information processing [24].

Recently, the field of associating ultracold atoms into molecules has received more interest [25,26] owing to the applications, ranging from research on BCS-BEC crossover [27–29] to the exploration of quantum phase transition [30]. In addition, the coupled atom-molecule systems have deep quantum optical analogies [31,32]. Bosonic molecules coupled to bosonic atoms is a matter-wave analog of parametric coupling of photons, which has important applications in

generating nonclassical light fields. Matter-wave bistability [33], periodic modulation effects on phase transitions [34], and virtual monopoles [35] in coupled ultracold atom-molecule quantum gases have been investigated. However, the dynamic stabilization of the systems has never been demonstrated. In this paper we explore the dynamic stabilization of a coupled bosonic atom-molecule system including many-body interactions between particles, which lead to the existence of an unstable equilibrium state. We stabilize the system to this state by employing a short-pulse phase-periodic modulation. We find that a long-pulse modulation will drive the system into high-amplitude periodic motions or chaotic motions. *In particular, we show that these mean-field results can be strongly modified when we take into account the effects of quantum fluctuations.*

II. MEAN-FIELD MODEL

We start from a three-mode model which describes the atom-heteronuclear molecule conversion with two atomic modes and one molecular mode. The basic assumption here is that the spatial wave functions for the three modes are fixed so that we can associate each mode with an annihilation operator \hat{a}_j of a particle in atomic mode $j = 1, 2$ or in molecular mode $j = m$. Under this approximation, the Hamiltonian takes the form [36]

$$\hat{H} = \Delta N_m + \sum_{i,j} \chi_{ij} N_i N_j + \eta (e^{-i\phi} \hat{a}_1^\dagger \hat{a}_2^\dagger \hat{a}_m + \text{H.c.}), \quad (1)$$

where the detuning Δ represents the energy difference between the molecular and the atomic modes, which can be tuned by an external field, $\eta e^{\pm i\phi}$ refers to the atom-molecule coupling, and $\chi_{ij} = \chi_{ji}$ denotes the interaction between mode i and mode j proportional to the s -wave scattering length. In this model, the total atom number $N = N_1 + N_2 + 2N_m$ ($N_j = \hat{a}_j^\dagger \hat{a}_j$) is a conserved quantity. Indeed, $D = \hat{a}_1^\dagger \hat{a}_1 - \hat{a}_2^\dagger \hat{a}_2$ is also a conserved quantity, which characterizes the particle-number imbalance between the two atomic modes. Note that the coupling parameter $\eta e^{i\phi}$ is complex. To achieve this, one can

*lsc1128lsc@126.com

split the laser pulse into two beams and then recombine and focus them on the system. As a result, the phase factor ϕ can be determined by the difference in optical paths between the two laser beams [37]. It should be mentioned that the above single-mode approximation concentrates on condensate modes only and neglects the effects of the particles occupying other modes, which is only valid at zero temperature [38] or when the energy distribution of the thermal particles characterized by $k_B T$ (k_B is the Boltzmann constant and T is the temperature) is much smaller than the effective coupling strength $\eta\sqrt{N}$ [39]. In the present study, we restrict our consideration to the symmetric case where the two atomic modes have the same particle number, i.e., $D = 0$. In this situation, the Hamiltonian can be simplified by using the conserved quantities. By neglecting the trivial constant terms, we have

$$\hat{H} = \chi N_m^2 + \beta N_m + \eta(e^{-i\phi}\hat{a}_1^\dagger\hat{a}_2^\dagger\hat{a}_m + \text{H.c.}), \quad (2)$$

where $\chi = \chi_{11} + \chi_{22} + \chi_{mm} + 2(\chi_{12} - \chi_{1m} - \chi_{2m})$ and $\beta = \Delta - N(\chi_{11} - \chi_{1m}) - 2N\chi_{12} - N(\chi_{22} - \chi_{2m})$. We assume that the phase $\phi(t) = \Delta\theta \cdot \delta_\tau$ is a periodic function of time, where $\delta_\tau = \delta(t - n\tau)$ is the δ function, with $n = 0, 1, 2, \dots$, and $\Delta\theta$ is the magnitude of phase shift when $t = n\tau$. We further suppose that the phase shift is turned on only at certain times of a period τ .

Subsequently, we use the mean-field approach to describe the system, which has been proven to be a powerful tool for the study of BECs. In this description, we can treat the operator \hat{a}_j as a complex number in Heisenberg's equation due to the bosonic nature of the particles, i.e., $\hat{a}_j \sim \sqrt{N}a_j$, and then the dynamical equations become ($\hbar = 1$)

$$i \frac{d}{dt} \begin{pmatrix} a_a \\ a_m \end{pmatrix} = \begin{pmatrix} 0 & \Omega e^{-i\phi} a_a^* \\ \frac{\Omega}{2} e^{i\phi} a_a & \beta + 2\alpha |a_m|^2 \end{pmatrix} \begin{pmatrix} a_a \\ a_m \end{pmatrix}, \quad (3)$$

where $a_a = a_1 = a_2$ means that the dynamical properties of two atomic modes are identical. The effective particle interaction and atom-molecule coupling are $\alpha = N\chi$ and $\Omega = \sqrt{N}\eta$, respectively. The normalization condition becomes $2(|a_a| + |a_m|) = 1$. Actually, in the large-particle-number limit, i.e., $N \gg 1$, the mean-field model, (3), gives a nice approximation of the quantum model, (1), with quantum fluctuations of order $1/N$ [40].

To simplify the problem, we express the complex variable a_l by its module and phase, i.e., $a_l = \sqrt{n_l}e^{i\theta_l}$, with $l = a, m$. Considering the fact that the system consists of two conserved quantities N and D , our problem can be described by two independent variables: the normalized population in the molecular mode $p = n_m \in [0, 1/2]$ and the relative phase $q = 2\theta_a - \theta_m$ between the atomic and the molecular modes. In this description, the normalized population in the atomic mode is $n_a = (1 - 2p)/2$. As a result, Eq. (3) can be expressed as

$$\frac{dp}{dt} = \Omega\sqrt{p(1-2p)^2} \sin(q + \phi), \quad (4)$$

$$\frac{dq}{dt} = \beta + 2\alpha p + \Omega \frac{1-6p}{2\sqrt{p}} \cos(q + \phi). \quad (5)$$

It is noted that the variables p and q in Eqs. (4) and (5) are canonically conjugate. With the help of $dp/dt = -\partial\mathcal{H}/\partial q$ and $dq/dt = \partial\mathcal{H}/\partial p$, we can obtain the corresponding

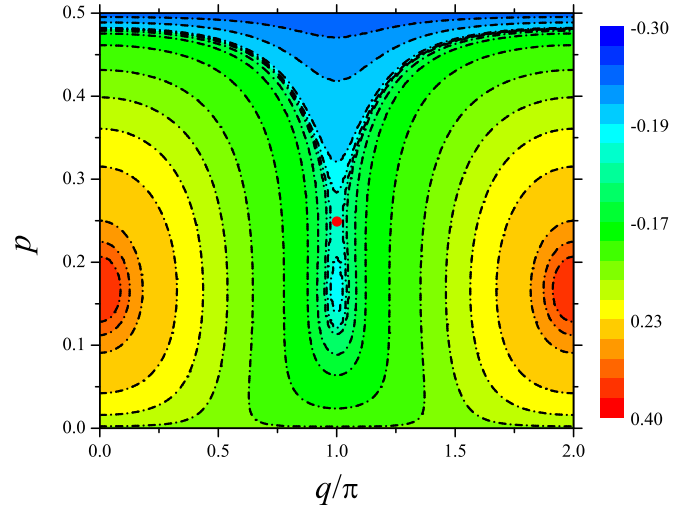


FIG. 1. (Color online) Classical energies and fixed point distribution in the (p, q) phase space with $\beta = \Omega = 1$ and $\alpha = -3$. The central filled (red) circle denotes the unstable saddle point $(1/4, \pi)$.

classical Hamiltonian as

$$\mathcal{H}(t) = \alpha p^2 + \beta p + \Omega\sqrt{p(1-2p)^2} \cos[q + \phi(t)]; \quad (6)$$

when $\phi = 0$, in a simple mechanical analogy, \mathcal{H} describes a nonrigid pendulum, of tilt angle q and length proportional to $\Omega\sqrt{p(1-2p)^2}$ that varies with p . It can be found that the nonlinearity of the system arises from two factors: the collisional particle interactions and the atom-molecule coupling. We denote the fixed points in the (p, q) phase space (\bar{p}, \bar{q}) , which can be determined by the equilibrium equations $dp/dt|_{(\bar{p}, \bar{q})} = dq/dt|_{(\bar{p}, \bar{q})} = 0$.

In a suitable range of parameter values, i.e., $-9\Omega^2(2 + \sqrt{3 + 9\Omega^2})/(-2 + 18\Omega^2) < \alpha < -(1 + \sqrt{2}\Omega)$, with $\beta = 1$, there are three stationary solutions of q with $q + \phi = \pi$. Further analysis shows that the middle solution is dynamically unstable and the other two are stable [36]. Such behavior is typical in bistable systems [41]. In Fig. 1, we illustrate the classical phase-space structure for $\beta = \Omega = 1$ and $\alpha = -3$. In this case, a saddle point, i.e., $(\bar{p}, \bar{q}) = (p_0 = 1/4, \pi)$, represents an unstable equilibrium state possessing an imaginary excitation frequency which gives a signature of dynamical instability or matter-wave bistability [33]. The existence of this point corresponds to the occurrence of a swallowtail loop structure for the mean-field energy levels [42], which can lead to the breakdown of adiabaticity of the tunneling [43] and the delocalization for the dynamics [44]. The unstable fixed point is located at the intersection of the lines $p = 1/4$ and $q = \pi$, and the trajectory passing through this point develops a separatrix that separates the whole classical phase space into three regions with different orbital motions. It should be mentioned that the fixed points in the classical phase space just correspond to the eigenstates of the mean-field model, (3). From this perspective the saddle point denotes a metastable eigenstate with local maximum energy and refers to a situation with a mixture of equal atoms and molecules (i.e., $2n_m = 2n_a = 1/2$).

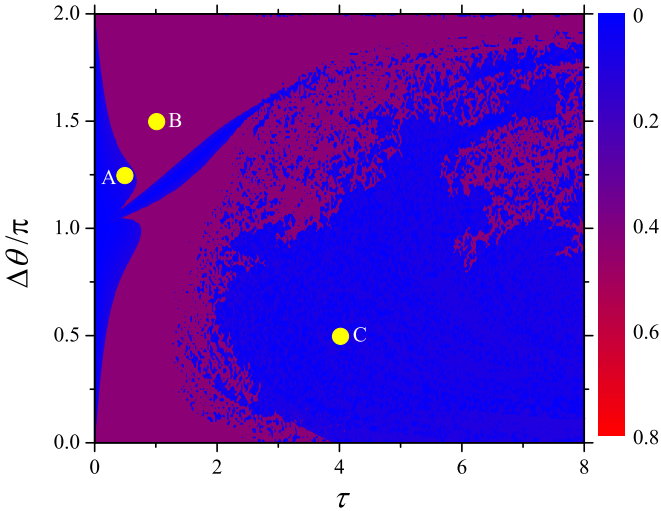


FIG. 2. (Color online) Map of the stability region for molecular population p after 100 of evolution. The stable region is dark blue and the unstable region is dark red. The results shown are the relative deviations $|\bar{p} - p_0|/p_0$ obtained from time-averaged calculations. A, B, and C indicate the modulation parameters used for the data in other figures.

III. DYNAMIC STABILIZATION

The numerical simulation begins from the unstable state (p_0, π) by employing the fourth- through fifth-order Runge-Kutta algorithm with an adaptive time step. Dynamic stabilization, expecting very small fluctuations of p_0 , can be achieved by using a periodic phase shift that denotes a sudden translation along the q direction in the classical phase space. We investigate the range of modulation periods and amplitudes that provides stabilization of the atom-molecule conversion dynamics. The calculated results are shown in Fig. 2, which displays a map of the stability region versus the modulation period τ and amplitude $\Delta\theta$. The stability criterion applied here is $|\bar{p} - p_0|/p_0 < 0.15$, with $\bar{p} = \int_0^t p dt' / \int_0^t dt'$, for more than 10 runs at 100 of evolution indicated by the dark-blue region corresponding to a nearly maximum atom-molecule (50:50) mixing state. In Fig. 2 we see that the stability region covers both short- and long-pulse periodic modulation and its area is almost as large as the instability region indicated in dark red.

To show the validity of the stability diagram obtained by using the time-averaged criterion, we demonstrate the time evolution of the molecular population p for different modulation parameters. Both case A and case C correspond to the time sequences indicated in the stability region. Case B is chosen to produce a more unstable condition. We find that in the modulated case (see Fig. 3), the period of the oscillation of p around p_0 is completely determined by the period of the modulation and the nonperiodicity of the oscillation increases with increasing modulation period. The heavy gray line showing the unmodulated evolution is given for comparison. In the unmodulated case, the period of Rabi oscillation from the initial state ($p'_0 = 0.25001$, $q = \pi$), which slightly deviates from the unstable fixed point, can be easily evaluated by making use of the conservation of the classical energy, (6), whose value is determined to be -0.1875

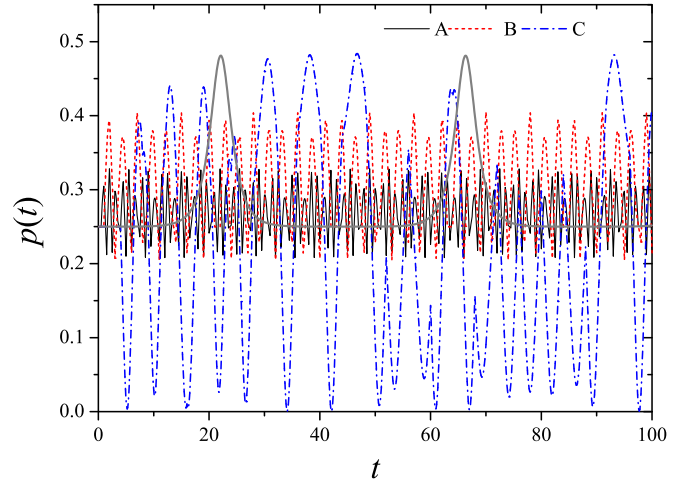


FIG. 3. (Color online) Evolution of p from p_0 for different modulation parameters $\Delta\theta$ and τ (cases A–C in Fig. 2). The thick gray line showing the unmodulated evolution is given for comparison.

from the initial condition. With the help of the expression $T_R = \oint |\partial q / \partial \mathcal{H}| dp = 2 \int_{p_0}^{p_{\max}} |\partial q / \partial \mathcal{H}| dp$, with p_{\max} corresponding to the maximum ($\doteq 0.4812$) of the reachable molecular population p , we obtain $T_R \doteq 42$ and find that it is in good agreement with the numerical results shown in Fig. 3. From the time evolutions, it can be seen that the dynamic stabilization works well in case A and the maximum fluctuation of p_0 (i.e., $|p(t) - p_0|$) is less than 0.08. However, in case B and case C the maximum deviations can reach 0.16 and 0.25, respectively. These results imply that in both these cases dynamical instability occurs. Unstable dynamics showing free evolution of atom-molecule conversion is not our goal. Obviously, the stability phase diagram illustrated in Fig. 2 based on the time-averaged criterion can not ensure dynamic stabilization during the whole time-evolution process.

For comparison, we calculate the maximum deviations from the initial value p_0 during the process of dynamical evolution with different modulation parameters. The maximum derivation is defined by $\delta p_{\max} = \max[|p(t) - p_0|/p_0]$ with the time range from 0 to 100. The dependence of δp_{\max} on both the modulation period τ and the amplitude $\Delta\theta$ is demonstrated in Fig. 4. We also adopt $\delta p_{\max} < 0.15$ as a stability criterion and then we find that the stability region is significantly reduced compared with that in Fig. 2. In particular, we see that the stability region in Fig. 4 only covers the range of modulation with short periods, which is very different from that in Fig. 2.

Similarly, we choose three typical points in Fig. 4, referring to three sets of modulation parameters, to show the validity of the stability diagram based on the maximum deviation criterion with the help of the time evolution of the molecular population p . The corresponding results are demonstrated in Fig. 5. Case A' is chosen to produce a stable condition, while case B' and case C' correspond to the time sequences indicated in the instability region. We see that in both the stable (A') and the weakly unstable (B') cases the atom-molecule conversion dynamics display periodic oscillations and the period is completely determined by the period of modulation. However, in the strongly unstable (C') case the atom-molecule

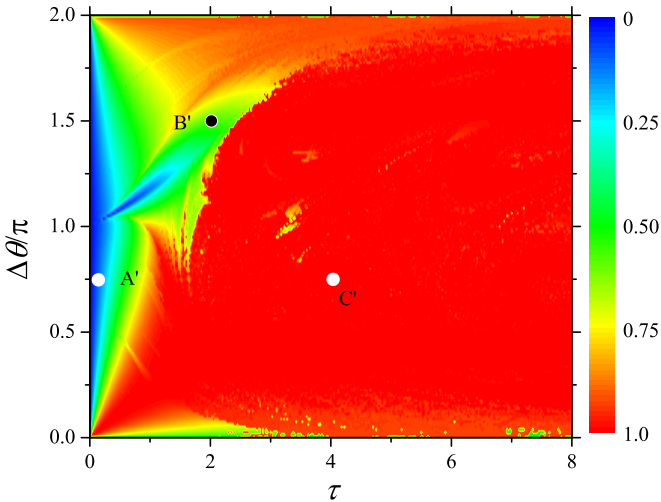


FIG. 4. (Color online) Map of the stability region for population p_0 after 100 of evolution. The stable region is blue and the unstable region is red. Results shown are the maximum deviations $\max[|p(t) - p_0|/p_0]$ during evolution. A', B', and C' indicate the modulation parameters used for the data in the other figures.

conversion dynamics show a nonperiodic stochastic motion. From the time evolutions, it can be found that the dynamic stabilization works well only in case A' and the maximum fluctuation of p_0 (i.e., $|p(t) - p_0|$) is less than 0.02. In case B' and case C' the maximum deviations can reach 0.15 and 0.25, respectively. Therefore, the stability diagram based on the maximum deviation criterion shown in Fig. 4 can ensure dynamic stabilization. In contrast to the stability diagram based on the time-averaged criterion, the range of modulation parameters for stability greatly decreases. For short-pulse modulation, the system can be stabilized over a wide range of modulation amplitudes.

The above results can be explained in terms of tracing the orbits of motion in the classical phase space. In Fig. 6 we illustrate two orbits starting from the same fixed point O and employing modulations with different periods and the

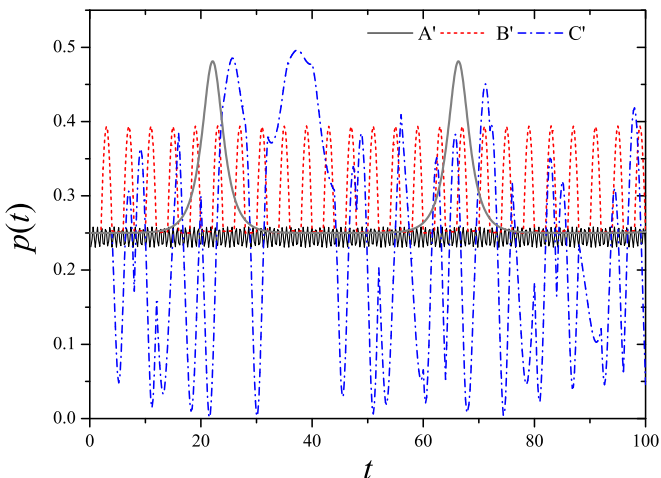


FIG. 5. (Color online) Evolution of p from p_0 for different modulation parameters $\delta\theta$ and τ (cases A', B', and C' in Fig. 4).

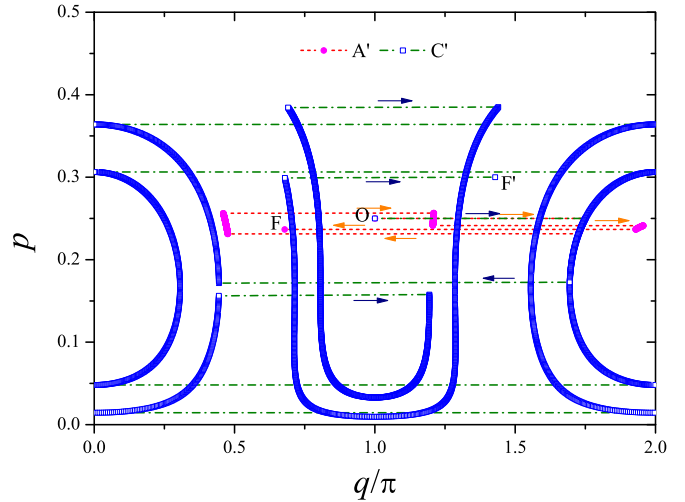


FIG. 6. (Color online) Traces of time evolution of an unstable point $(1/4, \pi)$ in phase space during the first five periods for different modulation parameters.

same amplitudes. For simplicity, we only show partial orbits corresponding to the first five periods of modulation. It is clear that, during every period of time evolution, for a short-pulse modulation (case A') the trajectory formed is very short and thus the derivation from p_0 is very small, while for a long-pulse modulation (case C') the trajectory formed is very long and thus a great derivation from p_0 is seen. It should be mentioned that all results of q are shown *modulo* 2π due to the periodicity of the classical phase space.

To see the overall dynamical characteristics, for the previous six cases we obtain the Poincaré section of the trajectories at moment $t = n\tau$, with n being an integer as shown in Fig. 7. From the modulation period τ it is easy to obtain the corresponding frequency ω_m . For cases A, B, C, A', B', and C', they are, respectively, $2\pi/0.5$, $2\pi/1$, $2\pi/4$, $2\pi/0.1$, $2\pi/2$,

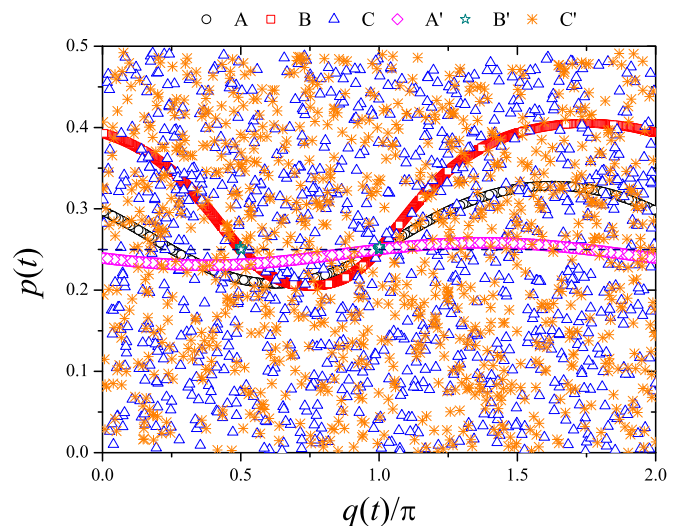


FIG. 7. (Color online) Poincaré section of the trajectories formed by evolving the system from the unstable point $(1/4, \pi)$ for different modulation parameters. Points plotted only at time $t = n\tau$. The dashed horizontal black line denotes $p_0 = 1/4$.

and $2\pi/4$. We can divide these cases into two classes by comparing the modulation frequency ω_m with the frequency of the intrinsic motion of the system, characterized by $\Omega = 1$. When $\omega_m \gg \Omega$ we denote them off-resonance cases, including cases A, B, A', and B'. When $\omega_m \sim \Omega$ we call them resonance cases such as cases C and C'. In the off-resonance cases, the snapshots of the orbits at multiple periods exhibit periodic motions; i.e., as evolution proceeds, the snapshots can link into lines (see cases A, B, and A') or repeat at some fixed points (see case B'). In the strong resonance cases, the dynamical behavior of the molecular population is very complicated due to the resonance between Rabi oscillation and periodic modulation. For different modulation parameters, it can be seen that p shows different behavior. In this situation we cannot find a periodic orbit as that in the off-resonance modulation cases. In Fig. 7 we see that the chaotic motion appears and one can verify this by calculating the maximum Lyapunov exponents [34].

IV. QUANTUM SIMULATION

In this section, we give a brief analysis beyond the mean-field description. The numerical simulations are based on the second quantized Hamiltonian, (2), with $D = 0$. We begin the analysis by writing Hamiltonian (2) in the Fock basis $|j, j, N - j\rangle$ (where j is the number of atoms in each atomic mode and $N - j$ is the number of particles in the molecular mode with $j = 0, 1, \dots, N$). Since the Hamiltonian conserves the total atom number N and $D = 0$, for $N = 2M$ it is convenient to adopt the so-called ‘‘pairs’’ basis $|n, M - n\rangle$ (where n and $M - n$ is the number of pairs of atoms in atomic and molecular modes, respectively, $n = 0, 1, \dots, M$). In this basis, the state of the system in vector form reads $\psi(t) = \sum_{n=0}^{M=N/2} C_n |n, M - n\rangle$ and the Hamiltonian can be written as a tridiagonal matrix, i.e., $H_{l,n} = \chi(M - n)^2 \delta_{l,n} + \beta(M - n) \delta_{l,n} + \eta e^{-i\phi} (n + 1) \sqrt{M - n} \delta_{l,n+1} + \eta e^{i\phi} n \sqrt{M - (n - 1)} \delta_{l,n-1}$, and the evolution equation becomes

$$i \frac{\partial}{\partial t} C_j = \sum_{l=0}^M H_{j,l} C_l. \quad (7)$$

For a fixed N , we evolve the system from a coherent state (i.e., Gross-Pitaevskii state) [40], $\psi(t=0) = \frac{1}{\sqrt{M!}} (aa^\dagger + ba_m^\dagger)^M = \sum_{l=0}^M \sqrt{\frac{M!}{l!(M-l)!}} (\sqrt{1-2p_0})^l e^{iq l} (\sqrt{2p_0})^{M-l} |l, M-l\rangle$, with $p_0 = 1/4$ and $q = \pi$, where a^\dagger is the atom-pair creation operator and $|0\rangle$ is the vacuum state. According to [40], the above coherent state corresponds to an eigenstate of the quantum system and the maximum difference in population probability between the two states is of the order $1/N$.

The quantum dynamical simulation is performed by numerical integration of Eq. (7). For the situation without modulation (see Fig. 8), it can be seen that the deviation of the time-average fraction of molecules from $2p_0$ decreases monotonically as the total atom number N increases at very short time evolution (e.g., $t = 2$). This verifies the validity of the mean-field description at the large-particle-number limit. However, when $t = 150$, the deviation will oscillate with N and this phenomenon reflects the effects of initial quantum fluctuations on the long time evolution.

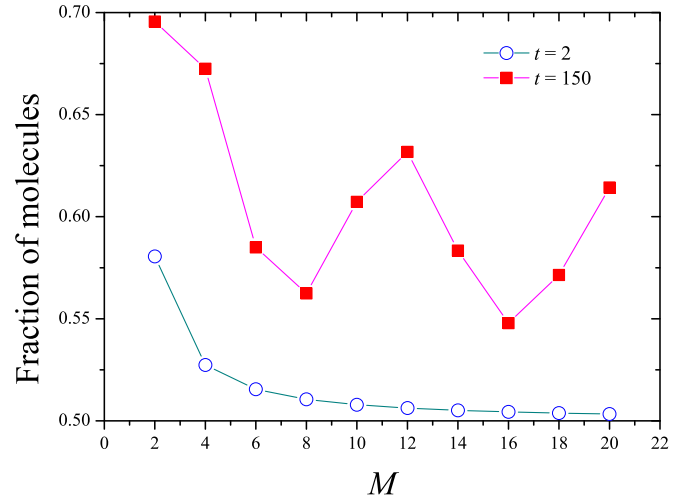


FIG. 8. (Color online) Quantum evolution results at $t = 2$ and $t = 150$ for different particle numbers $N = 2M$.

For the situation with modulation, we choose $N = 40$ as an example to show the dynamic stabilization when the system evolves at $t = 150$. In Fig. 9 we show the results for various modulation amplitudes and periods. Similarly to the mean-field case in Fig. 2, we also adopt the stability criterion $|\bar{p} - p_0|/p_0 < 0.15$ and indicate it by the dark-green and blue regions. Compared with the mean-field situation, two noticeable features are found: (i) the stability region only covers the supershort-pulse periodic modulation, and (ii) in the supershort-pulse region, there are instability regions, indicated in yellow and red, near the modulation amplitude $\Delta\theta = \pi$. The above results imply that in a finite quantum system the quantum fluctuations become very significant and the mean-field picture is not sufficient. However, the mean-field study can also

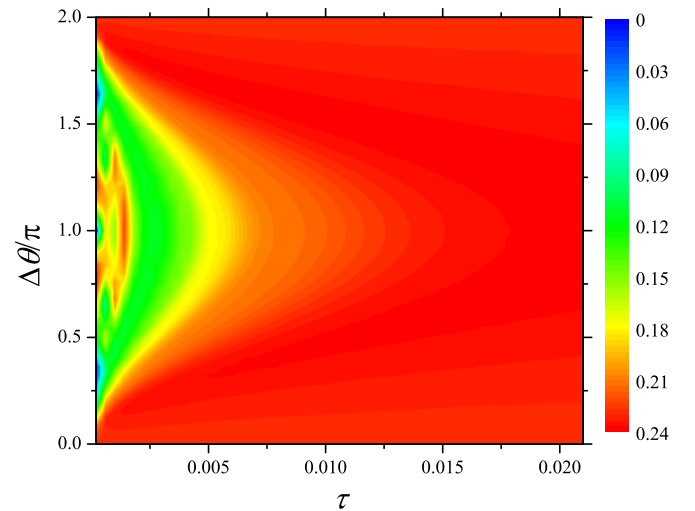


FIG. 9. (Color online) Map of the stability region from quantum evolution after 150 with $N = 40$. The stable region is dark green or blue, while the unstable region is yellow or red. Results shown are the relative deviations $|\bar{p} - p_0|/p_0$ obtained from time-averaged calculations.

provide important assistance in qualitative analysis of the corresponding quantum system.

V. CONCLUSION

In summary, we have numerically presented the dynamical stabilization of the atom-molecule conversion dynamics of ultracold bosonic quantum gases. In this study the many-body effect of the coherent particle interactions has been considered and a periodic phase modulation has been used to stabilize the system. In the mean-field treatment, we find that the unstable equilibrium state corresponds to a saddle point in the classical phase space, which can be dynamically stabilized by applying a short-pulse modulation. However, a long-pulse modulation will drive the unstable state in the instability region. In particular, when a strong resonance modulation is used the dynamical motion of the system will be chaotic. The stability diagram for the range of modulation periods and amplitudes that stabilizes the dynamics is given. We find that the stability

region obtained from the time-average calculation is very different from that based on a maximum absolute deviation analysis. By using the orbit tracking method, we show that the latter results are more believable, although the stability region greatly decreases in this situation. Finally, a brief quantum analysis is given and a qualitative agreement with the mean-field analysis is shown. In experiments, similarly to the quantum many-body spin-1 BEC [15,16], the binary BEC could be a promising candidate for verifying our theoretical analysis due to the advanced experimental techniques available in the fields of atomic and optical physics [45].

ACKNOWLEDGMENTS

This work was supported by the National Natural Science Foundation of China (Grant Nos. 11305120, 11275145, 91021021, and 11005055), the Natural Science Fundamental Research Program of Shaanxi Province of China (Grant No. 2015JQ1017), and the Fundamental Research Funds for the Central Universities of China.

-
- [1] G. P. Cook and C. S. Zaidins, *Am. J. Phys.* **54**, 259 (1986).
 - [2] M. Leibscher and B. Schmidt, *Phys. Rev. A* **80**, 012510 (2009).
 - [3] A. Stephenson, *Philos. Mag.* **15**, 233 (1908).
 - [4] M. Albiez, R. Gati, J. Fölling, S. Hunsmann, M. Cristiani, and M. K. Oberthaler, *Phys. Rev. Lett.* **95**, 010402 (2005).
 - [5] M.-S. Chang, Q. Qin, W. Zhang, and M. S. Chapman, *Nat. Phys.* **1**, 111 (2005).
 - [6] S. Levy, E. Lahoud, I. Shomroni, and J. Steinhauer, *Nature* **449**, 579 (2007).
 - [7] H. Saito and M. Ueda, *Phys. Rev. Lett.* **90**, 040403 (2003).
 - [8] H. Saito, R. G. Hulet, and M. Ueda, *Phys. Rev. A* **76**, 053619 (2007).
 - [9] R. L. Compton, Y.-J. Lin, K. Jiménez-García, J. V. Porto, and I. B. Spielman, *Phys. Rev. A* **86**, 063601 (2012).
 - [10] F. Kh. Abdullaev, J. G. Caputo, R. A. Kraenkel, and B. A. Malomed, *Phys. Rev. A* **67**, 013605 (2003).
 - [11] W. Zhang, B. Sun, M. S. Chapman, and L. You, *Phys. Rev. A* **81**, 033602 (2010).
 - [12] N. Bar-Gill, G. Kurizki, M. Oberthaler, and N. Davidson, *Phys. Rev. A* **80**, 053613 (2009).
 - [13] E. Boukobza, M. G. Moore, D. Cohen, and A. Vardi, *Phys. Rev. Lett.* **104**, 240402 (2010).
 - [14] F. Sols and S. Köhler, *Laser Phys.* **14**, 1259 (2004).
 - [15] C. S. Gerving, T. M. Hoang, B. J. Land, M. Anquez, C. D. Hamley, and M. S. Chapman, *Nat. Commun.* **3**, 1169 (2012).
 - [16] T. M. Hoang, C. S. Gerving, B. J. Land, M. Anquez, C. D. Hamley, and M. S. Chapman, *Phys. Rev. Lett.* **111**, 090403 (2013).
 - [17] A. Zenesini, H. Lignier, D. Ciampini, O. Morsch, and E. Arimondo, *Phys. Rev. Lett.* **102**, 100403 (2009).
 - [18] C. D. Hamley, C. Gerving, T. Hoang, E. M. Bookjans, and M. S. Chapman, *Nat. Phys.* **8**, 305 (2012).
 - [19] C. Gross, T. Zibold, E. Nicklas, J. Estève, and M. K. Oberthaler, *Nature (London)* **464**, 1165 (2010).
 - [20] M. F. Riedel, P. Böhi, Y. Li, T. W. Hänsch, A. Sinatra, and P. Treutlein, *Nature (London)* **464**, 1170 (2010).
 - [21] C. Gross, H. Strobel, E. Nicklas, T. Zibold, N. Bar-Gill, G. Kurizki, and M. K. Oberthaler, *Nature (London)* **480**, 219 (2011).
 - [22] B. Lucke *et al.*, *Science* **334**, 773 (2011).
 - [23] J. Ma, X. Wang, C. Sun, and F. Nori, *Phys. Rep.* **509**, 89 (2011).
 - [24] S. L. Braunstein and P. van Loock, *Rev. Mod. Phys.* **77**, 513 (2005).
 - [25] T. Köhler, K. Góral, and P. S. Julienne, *Rev. Mod. Phys.* **78**, 1311 (2006).
 - [26] E. A. Donley, N. R. Claussen, S. T. Thompson, and C. E. Wieman, *Nature (London)* **417**, 529 (2002).
 - [27] E. Timmermans, K. Furuya, P. W. Milonni, and A. K. Kerman, *Phys. Lett. A* **285**, 228 (2001); M. Holland, S. J. J. M. F. Kokkelmans, M. L. Chiofalo, and R. Walser, *Phys. Rev. Lett.* **87**, 120406 (2001).
 - [28] Q. Chen, J. Stajic, S. Tan, and K. Levin, *Phys. Rep.* **412**, 1 (2005).
 - [29] C. A. Regal, M. Greiner, and D. S. Jin, *Phys. Rev. Lett.* **92**, 040403 (2004).
 - [30] G. Santos, A. Foerster, J. Links, E. Mattei, and S. R. Dahmen, *Phys. Rev. A* **81**, 063621 (2010).
 - [31] M. W. Jack and H. Pu, *Phys. Rev. A* **72**, 063625 (2005).
 - [32] I. Tikhonenkov, E. Pazy, Y. B. Band, and A. Vardi, *Phys. Rev. A* **77**, 063624 (2008); M. Ögren, C. M. Savage, and K. V. Kheruntsyan, *ibid.* **79**, 043624 (2009).
 - [33] L. Jiang, H. Pu, A. Robertson, and H. Y. Ling, *Phys. Rev. A* **81**, 013619 (2010).
 - [34] S. C. Li and L. C. Zhao, *J. Opt. Soc. Am. B* **31**, 642 (2014).
 - [35] S. C. Li, L. B. Fu, and J. Liu, *Phys. Rev. A* **89**, 023628 (2014).
 - [36] L. Zhou, W. Zhang, H. Y. Ling, L. Jiang, and H. Pu, *Phys. Rev. A* **75**, 043603 (2007).

- [37] F. Cui and B. Wu, *Phys. Rev. A* **84**, 024101 (2011).
- [38] C. P. Search and P. Meystre, *Phys. Rev. Lett.* **93**, 140405 (2004).
- [39] J. Liu, B. Liu, and L. B. Fu, *Phys. Rev. A* **78**, 013618 (2008).
- [40] S. C. Li and L. B. Fu, *Phys. Rev. A* **84**, 023605 (2011).
- [41] H. M. Gibbs, *Controlling Light with Light* (Academic Press, Orlando, FL, 1985).
- [42] S. C. Li and L. C. Zhao, *Europhys. Lett.* **104**, 66002 (2013).
- [43] J. Liu, B. Wu, and Q. Niu, *Phys. Rev. Lett.* **90**, 170404 (2003); H. Pu, P. Maenner, W. Zhang, and H. Y. Ling, *ibid.* **98**, 050406 (2007).
- [44] G. Santos, A. Tonel, A. Foerster, and J. Links, *Phys. Rev. A* **73**, 023609 (2006).
- [45] J. Ruseckas, G. Juzeliūnas, P. Öhberg, and M. Fleischhauer, *Phys. Rev. Lett.* **95**, 010404 (2005).